

[Purchase  
Information](#)

[Information  
pour  
acheter](#)

[Titles  
Titres](#)

[←  
Article](#)

[→  
Article](#)



**Geological Survey  
of Canada**

**CURRENT RESEARCH  
2001-C24**

***Evaluating the potential for three-dimensional  
structural modelling of the Archean and  
Paleoproterozoic rocks of central Baffin Island,  
Nunavut***

***E.A. de Kemp, D. Corrigan, and M.R. St-Onge***



Natural Resources  
Canada

Ressources naturelles  
Canada

Canada

# CURRENT RESEARCH RECHERCHES EN COURS 2001

Purchase  
Information

Information  
pour  
acheter

Titles  
Titres

←  
Article

→  
Article



©Her Majesty the Queen in Right of Canada, 2001  
Catalogue No. M44-2001/C24E-IN  
ISBN 0-662-29879-9

Available in Canada from the  
Geological Survey of Canada Bookstore website at:  
<http://www.nrcan.gc.ca/gsc/bookstore> (Toll-free: 1-888-252-4301)

A copy of this publication is also available for reference by depository  
libraries across Canada through access to the Depository Services Program's  
website at <http://dsp-psd.pwgsc.gc.ca>

Price subject to change without notice

**All requests for permission to reproduce this work, in whole or in part, for purposes of commercial use, resale, or redistribution shall be addressed to: Earth Sciences Sector Information Division, Room 200, 601 Booth Street, Ottawa, Ontario K1A 0E8.**



## **Evaluating the potential for three-dimensional structural modelling of the Archean and Paleoproterozoic rocks of central Baffin Island, Nunavut**

***E.A. de Kemp, D. Corrigan, and M.R. St-Onge***

*Continental Geoscience Division, Ottawa*

*de Kemp E.A., Corrigan D., and St-Onge, M.R., 2001: Evaluating the potential for three-dimensional structural modelling of the Archean and Paleoproterozoic rocks of central Baffin Island, Nunavut; Geological Survey of Canada, Current Research 2001-C24, 17 p.*

### **Abstract**

*The Archean and Paleoproterozoic rocks of western central Baffin Island are being mapped at 1:100 000 scale at the exposed topographic surface. This data is being used to create three-dimensional (3D) structural models of key lithotectonic boundaries and associated deformation fabrics. Initial field investigations indicate extensive basement involvement during Paleoproterozoic deformation, along with folding and thrusting of cover rocks. Three-dimensional modelling of the complex structures produced by these processes would help extend our geological interpretations, now confined to 2D models in the form of geological maps, into the subsurface, thus helping to constrain the tectonic framework in this northern margin of the Trans-Hudson Orogen. Three-dimensional modelling activity is focused on extending the geometry of the basement (Archean) / cover (Paleoproterozoic) boundary, vergence mapping of regional folds and faults developed in the upper sequence of the Piling Group (Longstaff Bluff Formation), and the high-resolution 3D mapping of the base of the mafic volcanic Bravo Lake Formation.*



## Résumé

*Un projet de cartographie à l'échelle de 1/100 000 des roches affleurantes de l'Archéen et du Paléoproterozoïque est en cours dans la partie centre ouest de l'île de Baffin. Les données recueillies sont utilisées pour créer des modèles structuraux tridimensionnels des principales frontières lithotectoniques et des textures de déformation qui leur sont associées. Les premières études de terrain indiquent que le substratum a été grandement affecté par la déformation paléoproterozoïque, événement qui a été accompagné du plissement et du charriage des roches de couverture. La modélisation tridimensionnelle des structures complexes aidera à ajouter la profondeur aux interprétations géologiques qui, pour le moment, se limitent à des modèles bidimensionnels sous la forme de cartes géologiques. Ces éléments d'information contribuent à circonscrire le cadre tectonique de la marge septentrionale de l'orogène trans-hudsonien. La modélisation tridimensionnelle vise essentiellement à approfondir la géométrie de la frontière entre le substratum (Archéen) et la couverture (Paléoproterozoïque), la cartographie de la vergence des failles et des plis régionaux qui se sont formés dans la séquence supérieure du Groupe de Piling (Formation de Longstaff Bluff) et la cartographie tridimensionnelle à haute résolution de la base de la Formation de Bravo Lake (roches volcanomafiques).*

## INTRODUCTION

Recently developed approaches to the construction of 3D geological models facilitate the inclusion of field-based data from regional mapping programs (de Kemp 1998, 1999, 2000a, b; de Kemp and Sprague, 2001). These methods are now being applied in the context of the central Baffin Island bedrock 1:100 000 scale mapping project. This report outlines the initial phase of 3D modelling of the bedrock geology of the central Baffin Island with a brief summary of the relevant structural elements that affect 3D modelling. Our aim in creating these models, which are essentially 3D maps, is to provide visual



and testable models that supplement and perhaps enhance the 2D geological map interpretation. Collectively, all our models, whether they are 3D or 2D geological maps, are aids to better articulate and understand the tectonic history during crustal assemblage of the Trans-Hudson Orogen in this region.

## GENERAL GEOLOGY

The Trans-Hudson Orogen on central Baffin Island is dominated by a roughly east-west-trending fold and thrust belt, referred to as the Foxe Fold Belt (Jackson, 1969, 1978; Morgan et al., 1976). The northern margin of this belt is composed of reworked Archean basement (Rae Province); a thin unconformably overlying parautochthonous lower sequence of quartzite and marble (Dewar Lakes and Flint Lake formations, respectively, of the Piling Group); an upper foredeep sequence (Astarte River and Longstaff Bluff formations); a series of allochthonous mafic volcanic units (Bravo Lake Formation); and a metamorphic-plutonic southern border zone.

The contact between Archean basement and Paleoproterozoic cover is rarely exposed as an unconformity, and is predominantly intruded by biotite syeno- to monzogranite plutons that mask pre-existing depositional and/or tectonic relationships. Four main tectonothermal episodes affected the rocks in the region. The earliest an Archean mid-amphibolite-facies event ( $D_{1A}$ ) followed by two Paleoproterozoic compressional events ( $D_{1P}$  and  $D_{2P}$ ) and a cross-folding ( $D_{3P}$ ) event, which produces type 1 interference (Ramsay, 1967), basement-cover culminations, and Bravo Lake Formation folded klippen in the southern border of the map area, Corrigan et al. (2001) and **Table 1**.



## STRUCTURAL GEOLOGY

The core of the Foxe Fold Belt is dominated by upright folded imbricates of Piling Group metaturbidites. Preliminary investigation of the style and history of Paleoproterozoic structures in the central part of the belt indicates that several ( $D_{1P}$ – $D_{3P}$ ) shortening pulses produced present-day geometries. Steep to overturned bedding and intersecting axial-plane fan cleavage produce classic patterns, typical of younger telescoped flysch basins (Bierman, 1987). Structural vergence direction changes both laterally along the deformation front, and perpendicular to the orogen. This indicates that tectonic mass transfer is not unidirectional, but confined to a narrow bipolar, roughly north-northwest to south-southeast displacement and east-northeast rotation axis.

Previous fieldwork in the most northwestern region of the map area, combined with U/Pb zircon and monazite geochronology (Bethune and Scammel, 1997), indicates that Archean rocks are extensive and that these rocks have been reworked by Paleoproterozoic northeast-trending folding and mid-amphibolite-facies overprinting (Jackson, 2000). Occurrences of outliers of lower-sequence Piling Group rocks (Dewar Lakes quartzite and Flint Lake formation marble) in the dominantly Archean northwestern region, indicates that the Archean basement was involved in thick-skinned deformation during Paleoproterozoic ( $D_{1P}$ – $D_{3P}$ ) tectonothermal events.

The focus of this study is the 3D modelling of structures affected by these Paleoproterozoic events. In order to properly assess the potential for 3D modelling, a field investigation was undertaken to examine the structural elements formed by, and affected by, this history throughout the region. A summary of structural elements, including geometry of bedding, cleavage, and foliations, as well as fold-hinge orientations throughout the region, reveals several regional-scale patterns that help characterize the structural deformation (**Fig. 1**).



The following is a summary of the field investigation with characteristic structural elements based on a north to south transect, mapped through the project area in 2000. Major headings in the text match the labels of equal-angle structural plots for the areas discussed. We discuss the types of 3D structural models that are being produced and present several example 3D models from along a 2 km wide cross-section located in **Figure 2**. A more detailed delineation of structural domains with a more complete structural analysis will follow upon completion of 1:100 000 scale compilation, due for release in 2001.

### *Northern gneiss (basement)*

Structural geometries in the north of the map area are dominated by northeasterly trending Archean ortho-gneiss and granitoid (**Fig. 1**). This trend is consistent with the northeast trend of the Archean granite-greenstone terrain to the northwest (Bethune and Scammel, 1997; Jackson, 2000). Relatively massive granite bodies in this northwestern region have been intruded by Neoproterozoic gabbro dykes (Bethune and Scamell, 1997), indicating that this area is underlain by Archean basement. These areas are important inasmuch they are affected by Trans-Hudson deformation and contain folded outliers of Piling Group Metasedimentary rocks that could be used to map the 3D form surface of the basement-cover contact. Several cross-sections through this northern region indicate that map scale (1:100 000) fold patterns, such as Archean orthogneiss and granite contacts in the basement gneiss, mimic the form surface of the enveloping basement-cover contact.

We aim to construct a field-constrained 3D model of the basement-cover contact in this area. At a minimum the surface, or series of surfaces, must conform to the map pattern and the dip values where this contact is exposed. This is a high-priority modelling target and will involve several interpretive steps. Attention will be paid to establishing tie-lines between adjacent sections and resolving topological conflicts.



## *Archean basement (inliers)*

In addition to extensive exposed basement in the northern gneissic regions, several basement culminations, likely Archean, have been previously identified in the southern parts of the map area (Jackson 1969, 1978; Henderson and Henderson 1994). Others have recently been reported in Corrigan et al. (2001) along with potential Archean basement regions near Flint Lake, in the north of the map area (Morgan, 1983; Morgan et al. 1975, 1976; Corrigan et al., 2001).

No distinguishing internal fabric distribution pattern is demonstrated by these potential basement areas near Flint Lake (**Fig. 1**), although a general northeast map pattern of the Flint Lake Archean candidates is present. This may reflect the northeasterly Archean granite-greenstone structural grain (Jackson, 2000, Bethune and Scammell, 1997) imposed by Paleoproterozoic refolding of Archean structures. These areas around Flint Lake are bounded by younger intrusive granite bodies that contain enclaves of basal Piling Group quartzite and marble. Field mapping of the geometry of the intrusive contacts with these potential basement inliers indicates contacts are generally transposed and concordant to fabric in the younger intrusions. The intrusive contacts tend to dip away from these areas, which would be consistent with a basement culmination. We await more accurate U-Pb Zircon age determination of individual plutons before more 3D models are constructed, but anticipate complex interference geometries as is indicated by the map patterns (Fig. 1) (*see section on Basal Piling Group (lower sequence)*). Field efforts have focused on increasing the 2D accuracy of these potential basement contacts.

Domal culmination fabric trajectories are indicated in the southern Archean inliers (*see Corrigan et al. (2001) indicating participation in  $D_{1P}/D_{2P}$  shortening and  $D_{3P}$  cross folding. Where fabric analysis indicates these domal culmination structures, (radial-divergent dip directions), it is a simple task to extend these contacts, similar to extending concentric strain envelopes around plutons (Guglielmo, 1993; Schwerdtner, 1984; de Kemp, 1999; de Kemp and Sprague (2001)).*





### *Basal Piling Group (lower sequence)*

Paleoproterozoic outliers, such as Flint Lake Formation rocks near Isortoq Fiord (Jackson 1978; Bethune and Scamell 1997) provide indications that the lower Piling Group formed an onlap sequence at least 150 km inland from the present Flint Lake margin. As the sediments of this basal unit are tight to isoclinally folded, the original passive onlap margin would have extended for at least twice that distance, approximately 300 km. Plutonic envelopes along the northern and southern structural margins of the Piling Group, both as older stratigraphic basement and as younger intrusive bodies (see Corrigan (2001)), have significant influence on the style of deformation in these areas. Dip directions of lower sequence quartzite and marble (Flint Lake Formation) tend to be steeper, and variably rotated, away from the central east-west trend of the Piling Group. In general, the northern margin is characterized by a more northeasterly rotation of the planar fabrics about shallow northeast plunging isoclinal folds. Syndeformational Paleoproterozoic granitoid intrusions (Corrigan et al., 2001) emplaced along the relict basin margin have produced locally heterogeneous structures that scatter the fabric elements and likely influence the formation of parallel-to-intrusion structural grain of  $S_2$  and  $L_2$  fabric during  $D_{2p}$ . A 1 km thick slice of this granitoid unit was interpreted using fabric data adjacent to the granite-Piling contacts (**Fig. 2**). The granite volume corresponds to two linked domes, one south, and one north of Flint Lake (**Fig. 3**). We are constructing several of these structural cross-sections across basal Piling Group rocks and will link these with tie-lines parallel to local fold axis.



## *Central Piling Group (upper sequence)*

Most of the Piling Group, now 70 to 100 km across strike, is composed of east-west-striking and variably dipping psammite, with minor semi-pelite and wacke (see description Corrigan et al. (2001), re: Longstaff Bluff Formation). Sedimentary facies within the Longstaff Bluff Formation includes medium-grained to granular feldspathic and volcanoclastic wacke, along with psammite-pelite couplets such as those at Longstaff Bluff and along the western coast. Despite this variation, at the scale of mapping (1:100 000), specific lithological units distinct enough to be used as structural markers were not recognized during the first summer of fieldwork. Consequently, fold structures tend to be better observed at a distance, for example from helicopter, or identified by airphoto interpretation. Commonly, local monoclinical structures are preserved along topographic ridges where they are well exposed. Valleys tend to be filled with boulders and talus that can mask important structural features. Regional fold geometry is interpreted during the compilation of adjacent traverse data.

Internal fabric in these rocks is displayed as a penetrative  $S_2$  biotite foliation and as a planar spaced fracture and axial-plane parallel cleavage. Determination of the orientation of depositional beds tends to be dependent on the ratio of pelitic or semi-pelitic to psammitic components. Where bimodal grain sizes in siliciclastic assemblages, such as in a-e type turbidite couplets, are present, outcrop-scale cleavage-diffraction patterns are available for top determinations (see Fig. 4). The angle between cleavage and bedding is often less than  $10^\circ$ , suggestive of tight to isoclinal folding. Cleavage bedding asymmetries tend to be consistent for tens of kilometres. More detailed investigation is planned to determine the spatial distribution and nature (fold hinges versus thrust faults) of asymmetry transitions.

A preponderance of steep ( $50^\circ$ – $80^\circ$ ) bedding dips in turbidite units that rotate about a narrow (north-northwest to south-southeast) axis, combined with truncated folds, and less commonly, short overturned fold limbs are characteristic of structurally shortened or telescoped flysch basins worldwide



(i.e. Bierman, 1987). A complete geometric restoration of the Piling Group is beyond the scope of this study, but our initial field study and previous work suggests that the Piling Group sustained a large degree of telescoping (Henderson et al. 1988, 1989; Morgan et al., 1975, 1976; Tippet, 1980). This basin appears to be effected by early  $D_{1P}$  thrusting ( $T_{1P}$ ), along with concomitant and subsequent steep folding (dips  $> 50^\circ$ , see **Fig. 1**) that could collectively amount to 50–70% shortening. This suggests that the original basin width could have been 200–300 km. A systematic mapping of vergence directions (3D direction of overfolding) is presently being undertaken. Preliminary indications are that vergence vectors are confined to a narrow bipolar, north-to-south, near-vertical plane with regional-scale vergence varying directions both parallel to and across the orogenic front.

Visualization of the present telescoped geometry of the Piling Group is a goal of this project. We are presently constructing extended bedding and cleavage traces using 3D structural ‘ribbons’ (de Kemp 2000a; de Kemp and Sprague, 2001). Ribbons act as visual aids while interpreting fold geometry and provide the equivalent of a form-surface trace in 3D. These models will be compared with models of the folded basement-cover contact. This should provide insight into fold development, vergence patterns, shortening estimates, and basement influence, if any, on cover rocks.

## MAFIC KLIPPEN

**V**olcanic flow orientations within mafic to ultramafic metavolcanic klippen (Corrigan et al., 2001) near Nadluardjuk Lake display characteristic shallow dips ( $< 45^\circ$ ) in upright fold structures (Fig. 1). The base of this klippen is dominated by a several-metre-wide tectonic mélange (Raymond, 1975; H.H. Helmstaedt, pers. comm., 2000). Dip directions in the allochthonous rocks above the mélange surface form a great-circle distribution with a rotation axis oriented in a east-northeasterly direction. They differ by about  $15^\circ$  clockwise from the principal east-west bedding rotation axis within the Piling Group.



Interference fold patterns from  $D_{2P}$ – $D_{3P}$  superposed folding are readily observed from Landsat imagery and airphotos. The patterns define the outlines of these klippen and are expressed as several isolated structural keels across the southern margin of the map area.

A simple structural section through the most prominent of these mafic bodies is depicted in **Figure 5** with a preliminary 3D structural form surface (**Figure 6**). For methods used to construct these surfaces see de Kemp and Sprague (2001). Flatter, upright ( $D_{2P}$ ) folding combined with shallow thrusting ( $D_{1P}$ ) of mafic volcanic (Bravo Formation) klippen along the southern margin of the Piling Group may indicate that much of the regional shortening strain in the southern part of the belt was partitioned through thrusting. Determination of timing, direction, and tectonic transport of the klippen is yet to be determined.

### *Southern Piling Group (upper sequence)*

The southern border of the Piling Group (upper sequence) is dominated by mid- to upper-amphibolite (garnet-cordierite-sillimanite-K-feldspar) shallow-dipping beds displaying Type-1 ( $F_2$ – $F_3$ ) (Ramsay, 1967) interference folds. A structural plot (equal-angle) of main fabrics in this area seems superficially the same as the main core of the Piling Group to the north (**Fig. 1**). Field evidence from outcrop-scale folding, however, suggests that there should be an overall increase in contribution by  $D_{3P}$ – $F_3$  structures that have been observed as moderately northwest- to southeast-plunging tight upright folds. Regional-scale map patterns in the southern area also suggest that northwest- to southeast-trending folds have a significant effect on the area. Either  $F_3$  structures are components of both structural plots (northern and southern Piling Group) and field evidence for these structures is more available in the southern area, perhaps due to better exposure, or  $F_3$  structures are not well represented in the southern structural plot. These  $F_3$  structures, if present in the northern core region of the Piling Group, are not well preserved. This is



enigmatic, since  $F_3$  structures with similar orientations also are preserved in the lower sequence Piling Group along the northern Flint Lake area. As mentioned in the central Piling Group (upper sequence) section, there are few available marker units in the central areas where fold geometry is interpreted during the compilation stage.

The simple upright geometry of folds in this southern area facilitates the construction of 3D sections and 3D form-surface models, with the existing data (de Kemp, 2000a). Comparison of the modelled, 3D bedding surfaces between northern, and higher-grade southern regions of the Piling Group may provide insight into  $F_3$  effects throughout the upper sequence Piling Group.

## CUMBERLAND BATHOLITH AND S-TYPE PLUTONS

Syndeformational and postdeformational Paleoproterozoic granitoid bodies, including the Cumberland Batholith, are dominant in higher amphibolite-grade rocks in the southern margin of the map area (Corrigan et al. (2001)). These granitoid rocks were emplaced during major shortening ( $D_{1P}/D_{2P}$ ) of Piling Group metasedimentary rocks. The structural plot of foliation dip directions and fold-hinge orientations from the Cumberland Batholith rocks and younger S-type, two-mica, garnet-bearing leucogranite, indicates an asymmetric distribution, with a lack of westerly dipping fabrics (**Fig. 1**). Shallow ( $< 30^\circ$ ) to near-horizontal fold plunges to the northeast contrast with a symmetric fabric distribution in the upper sequence Piling Group sedimentary rocks, which have shallow westerly and easterly plunging fold hinges. This may be a result of the combined plotting of the syn- $D_{1P}$  Cumberland Batholith rocks, which contains deformed Piling Group enclaves and some syn- to late- $D_{2P}$  stage leucogranite suite rocks. Alternatively,  $D_{3P}$  structures in this region are poorly developed, producing only slight rotation of previous fabric  $S_2/L_2$  elements.



Geometric modelling of the southern S-type plutons and the margins of the Cumberland Batholith is a lower priority modelling target. These intrusive bodies have irregular margins that require a high degree of ground control to model. Also, it is not clear what a constrained geometric model of these bodies could contribute to furthering our tectonic understanding of the area. As our knowledge of the emplacement and strain history of these rocks improves, perhaps there will be a need to construct some models in this dominantly intrusive area.

## DISCUSSION

The preceding summary of structural features throughout the map area highlights the structural complexity that will need to be taken into account while constructing 3D models in this region. Unconformable boundaries, polyphase folding, thrusting, and crosscutting intrusive contacts are typical of this and other ancient orogenic belts throughout the shield areas of the world. Our aim is to pursue an integrated 3D interpretation which will evolve along with our understanding of the geologic history of the area.

A major goal of this component of the central Baffin bedrock mapping project is to characterize the regional scale 3D geometry of the Piling Group cover rocks and Archean basement contact. This surface can provide us with a tectonic marker or datum that tracks the composite effects of Paleoproterozoic deformation over a wide area. Identification, delineation, and the linking of pre-existing geology to the basal sequence Piling Group throughout the map area will be the first step in this process. To a certain extent this has already been done through geochronology (Bethune and Scamell, 1997) and recognition of basement unconformities and Piling Group outliers (Jackson, 2000; Corrigan et al., 2001). Detailed geometric examination of the basement-cover boundary and characterization of the contact relationships (unconformity, fault, intrusive, transposed) will be undertaken in future fieldwork.



Determination of structural vergence directions throughout the belt will likely result in a 3D structural vergence map that will help determine crustal-scale boundary conditions between the stable lower-plate paleomargin (Archean Basement + lower Piling Group paralochothon) and incoming upper plate (upper Piling and allochthonous Bravo Lake Formation) interaction.

One of the most difficult tasks in geological mapping is to determine the geometric relationships between local observations and regional structures (de Kemp, 2000b; Schetselaar 2000). This problem has an impact on methods used for 3D modelling: for example, modelling of pluton margins using adjacent structural observations rather than direct 3D mapping (de Kemp 1999) in higher relief areas. Establishing the geometric relationship between foliation and cleavage-fabric trajectories of lower sequence Piling Group rocks adjacent to the larger plutons, and the actual geometry of pluton boundaries will be important as these local observations could be used in 3D modelling of the larger contact surfaces. From this summer's field research, fabrics in the lower-sequence quartzite and marble consist of a composite transposed fabric that is parallel to the pluton boundary. Future work will continue to verify this relationship, which, if it continues to hold true, will be useful in controlling 3D ribbon geometry with individual structural observations. Other modelling 'targets' such as the basement-cover surface may or may not have appropriate structural point observations to constrain regional interpretations. However, regional 3D geometry can still be interpreted based on estimates that conforms to the 2D map patterns.

Where local planar and linear structural data provide poor support for the larger scale geometry modelling, other techniques will be used. The Bravo Formation is a prime candidate for this type of modelling as it appears to have a moderately folded, simple keel-like tectonic mélangé as the basal surface, in higher relief terrain. The geological surfaces in these situations can be modelled using geometric filters based on the classic three-point solution (De Paor, 1991), provided that topographic relief is of a higher order roughness than the geological surfaces being modelled (de Kemp, 1999). We will be involved in more detailed mapping and strain characterization of the klippen boundaries of the Bravo Formation in the



southern map area. A 20 m resolution, digital elevation model (DEM) is being constructed from SPOT satellite stereo pairs (Krupnik, 2000) for higher relief areas in the Nadluardjuk Lake area, in aid of this type of 3D mapping. Integrating the DEM and accurate positioning of the klippen contact should facilitate computation of structural orientation at ground level. These computed orientations could then be compared with adjacent structural field observations that can only help to further the overall structural analysis.

## CONCLUSIONS

The major conclusion from this preliminary work is that there is good potential for the construction of field-constrained, regional 3D models in the Foxe Fold Belt. We acknowledge the importance of obtaining both high-accuracy spatial information from fieldwork, and of learning the structural context prior to creating regional geological models. This integrated approach, we believe, will enhance our ability to produce communicative models that articulate and enhance our understanding of this part of the Trans-Hudson Orogen.

Initial field investigations summarized herein and Corrigan et al. (2001) indicate that a more detailed structural analysis of key boundaries and fabric elements, along with the 3D mapping of specific fold and thrust structures, could add significantly to constraining the regional tectonic framework. Special attention should be paid to increasing 3D accuracy of fabric trajectories and key lithotectonic contacts (eg. Basal Bravo Lake klippen); 3D vergence mapping throughout the belt to help constrain plate-margin interaction in the context of larger tectonic framework, i.e. St-Onge et al. (1999); and delineation and characterization of the northern margin basement-cover contact.





## REFERENCES

### **Bierman, C.**

1987: Basement topography and thrust fault ramping, a model to explain cleavage fans in the Mosel area (Rheinische Schiefergebirge), *Geologie en Mijnbouiw*, v. 66, p.333–341.

### **Bethune, K.M. and Scammell, R.J.**

1997: Legend and descriptive notes, Koch Island area, District of Franklin, Northwest Territories, (Part of NTS 37 C), Geological Survey of Canada, Open File 3391, scale 1:50 000.

### **Corrigan, D., Scott, D.J., and St-Onge, M.R.**

2001: Geology of the northern margin of the Trans-Hudson Orogen (Foxe Fold Belt), central Baffin Island, Nunavut; Geological Survey of Canada, Current Research 2001-B05.

### **de Kemp, E.A.**

1998: Variable 3-D geometrical projection of curvilinear geological features through direction cosine interpolation of structural field observations; *Computers and Geosciences*, v. 24, no. 3, p. 269–284.

1999: Visualization of complex geological structures using 3-D Bézier construction tools; *Computers and Geosciences*, v. 25, no. 5, p. 581–597.

2000a: 3-D visualization of structural field data: Examples from the Archean Caopatina Formation, Abitibi greenstone belt, Québec, Canada; *Computers and Geosciences*, v. 26, p.509–530.

2000b: Three-dimensional integration and visualization of structural field data: Tools for regional subsurface mapping; Ph.D. thesis, Université du Québec à Chicoutimi, 181 p.

### **de Kemp, E.A. and Sprague, K.**

2001: New interpretive tools for 3D structural geological modelling: Bézier based curves, ribbons and skeletons; Geological Survey of Canada, Current Research 2001-D22.

### **De Paor, D.G.**

1991: A modern solution to the classical 3-point problem; *Journal of Geological Education*, v. 39, p. 322–324.

### **Guglielmo G., Jr.**

1993: Interference between pluton expansion and non-coaxial tectonic deformation: three-dimensional computer model and field implications; *Journal of Structural Geology*, v. 15, p. 593–608.



**Henderson, J.R. and Henderson, M.N.**

1994: Geology of the Dewar Lakes area, central Baffin Island, District of Franklin, N.W.T. (parts of 27B and 37A); Geological Survey of Canada, Open File 2924, scale 1:100 000.

**Henderson, J.R., Grocott, J., Henderson, M.N., Falardeau, F., and Heijke, P.**

1988: Results of field work near Dewar Lakes, Baffin Island, N.W.T.; *in* Current Research, Part C, Geological Survey of Canada; Paper 88-1C, p. 101–108.

**Henderson, J.R., Grocott, J., Henderson, M.N., and Pereaault, S.**

1989: Tectonic history of the Lower Proterozoic Foxe–Rinkian Belt in central Baffin Island, N.W.T.; *in* Current Research, Part C, Geological Survey of Canada; Paper 89-1C, p. 186–187.

**Jackson, G.D.**

1969: Reconnaissance of north-central Baffin Island; *in* Report of Activities, Part A; Geological Survey of Canada; Paper 69-1A, p. 171–176.

1978: McBeth gneiss dome and associated Piling Group, central Baffin Island, District of Franklin; *in* Rubidium-Strontium Isotopic Age Studies, Report 2, (ed.) R.K. Wanless and W.D. Loveridge; Geological Survey of Canada; Paper 77-14, p. 14–17.

2000: Geology of the Clyde–Cockburn Land map area, north-central Baffin Island, Nunavut; Geological Survey of Canada, Memoir 440, 303 p.

**Krupnik A.,**

2000: Accuracy assessment of automatically derived digital elevation models from SPOT images; *Photogrammetric Engineering & Remote Sensing*, v. 66, no. 8, p. 1017–1023.

**Morgan, W.C.**

1983: Lake Gillian, District of Franklin, Northwest Territories; Geological Survey of Canada, Map 1560A, scale 1:250 000.

**Morgan, W.C., Bourne, J., Herd, R.K., Pickett, J.W., and Tippett, C.R.**

1975: Geology of the Foxe Fold Belt, Baffin Island, District of Franklin; *in* Report of Activities, Part A; Geological Survey of Canada, Paper 75-1A, p. 343–347.

**Morgan, W.C., Okulitch, A.V., and Thompson, P.H.**

1976: Stratigraphy, structure and metamorphism of the west half of the Foxe Fold Belt, Baffin Island; *in* Report of Activities, Part A; Geological Survey of Canada, Paper 76-1A, p. 387–391.

**Ramsay, J.G.**

1967: Folding and fracturing of rocks; McGraw-Hill, New York, 568 p.

**Raymond, L.A.**

1975: Tectonite and mélange – a distinction, *Geology*, v. 3, p.7–9.

**Schetselaar, E.M.**

2000: Integrated analyses of granite-gneiss terrain from field and multisource remotely sensed data: a case study from the Canadian Shield; Ph.D. thesis, Institute for Aerospace Survey and Earth Sciences (ITC) Netherlands, ITC dissertatie 73, p. 269.

**Schwerdtner, W.M.**

1984: Foliation patterns in large gneiss bodies of the Archean Wabigoon Subprovince, southern Canadian Shield, *Journal of Geodynamics*, v. 1, p.313–337.

**St-Onge, M.R., Lucas, S.B., Scott, D.J., and Wodicka, N.**

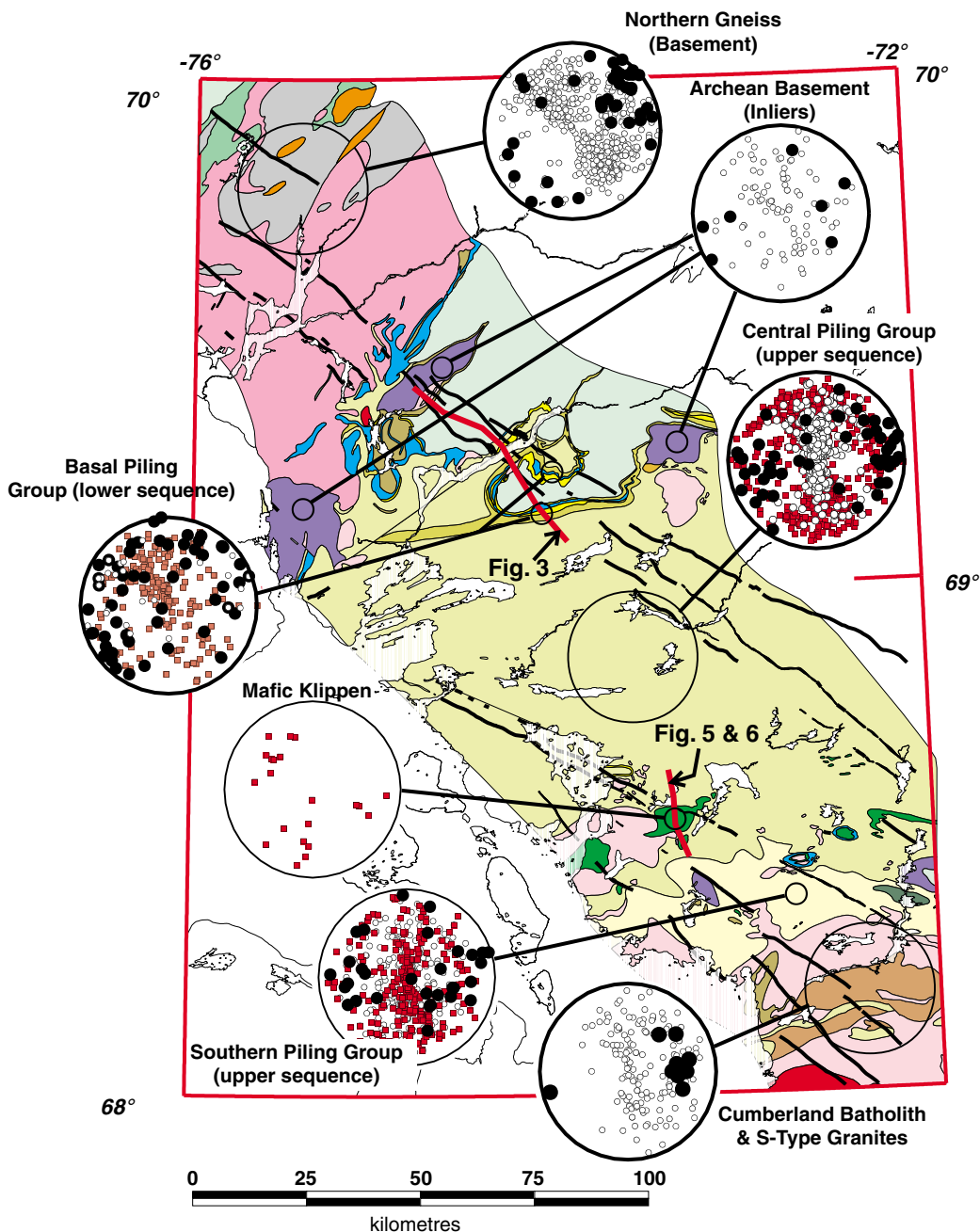
1999: Upper and lower plate juxtaposition, deformation and metamorphism during crustal convergence, Trans-Hudson Orogen (Quebec–Baffin segment), Canada; *Precambrian Research*, v. 93, p. 27–49.

**Tippett, C.R.**

1980: A geological cross-section through the southern margin of the Foxe Fold Belt, Baffin Island, Arctic Canada, and its relevance to the tectonic evolution of the northeastern Churchill Province; Ph.D. thesis, Queen's University, Kingston, Ontario, 409 p.

---






Geological Survey of Canada Project PS1006 EK



**Figure 1.** Equal-angle structural plots of bedrock structural-fabric elements in the western portion of the Foxe Fold Belt in central Baffin Island. Squares represent dip directions of bedding, open circles represent dip directions (on plane — 3D dip vectors) of cleavage, foliation, or gneissosity. Black-filled circles represent major fold-hinge lines. See text for summaries of each area. For map unit descriptions see Corrigan et al. (2001).




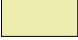




## Legend for Figure 1

### Archean





-  Granodiorite-monzogranite
-  Granitoid rocks and migmatite
-  Amphibolite
-  Tonalite gneiss
-  Possible Archean inliers (includes Proterozoic biotite syenogranite)



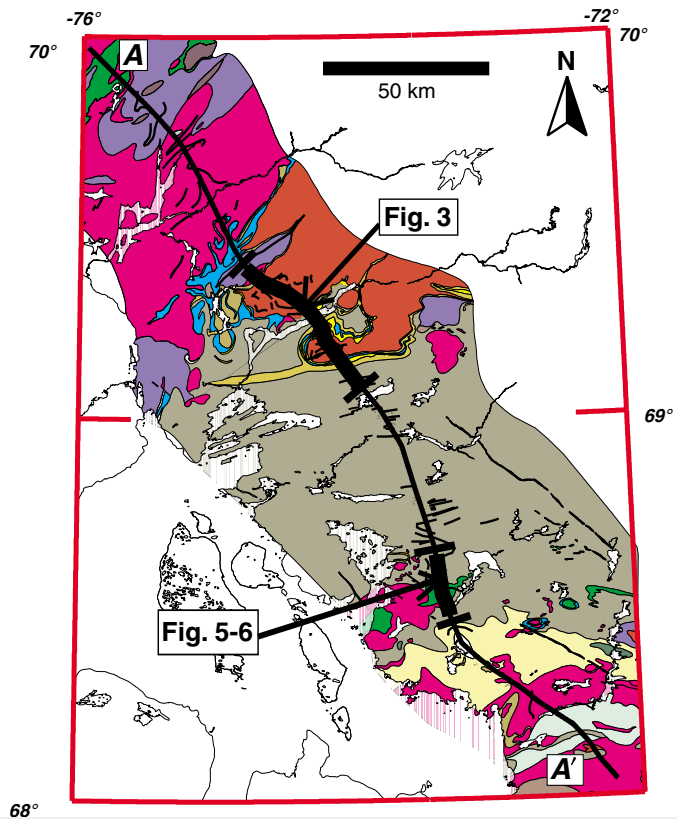
### Piling Group

- Bravo Lake Formation
  -  Mafic metavolcanic rocks, mafic ultramafic sills
-  Thrust fault
- Longstaff Bluff Formation
  -  Sillimanite-K-feldspar facies
  -  psammite-semipelite, wacke
- Astarte River Formation
  -  Fe-rich pelites
- Flint Lake Formation
  -  marble, calc-silicate rock
- Dewar Lakes Formation
  -  psammite
  -  quartzite

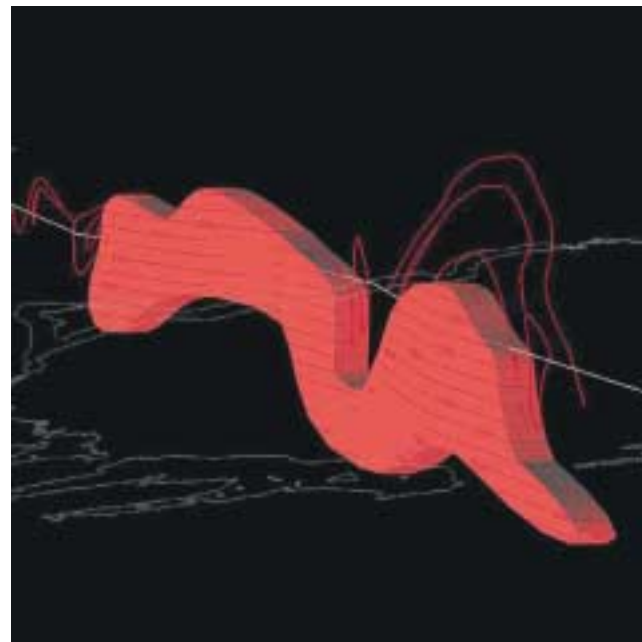
### Proterozoic Intrusions

-  Franklin dykes (ca. 750 Ma)
-  Biotite syenogranite
-  Two-mica S-type granite, diatexite (garnet + cordierite)
-  Megacrystic granite/granodiorite (Cumberland Batholith)





**Figure 2.** Location of interpretive cross-sections from Arcview GIS, parts of which are modelled in gOcad for Figures 3,5, and 6.



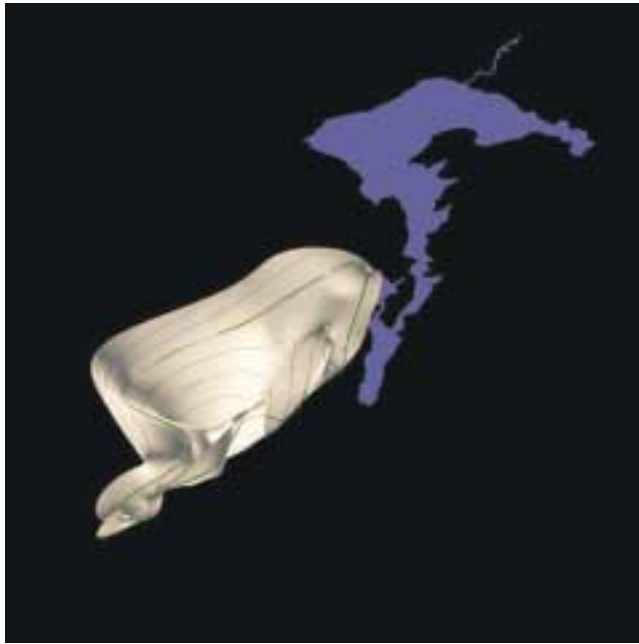
**Figure 3.** Perspective view of preliminary subsurface interpretation along section line depicted in Figure 2. Perspective view looking east-northeast.



**Figure 4.** Depositional bedding intersection with diffraction cleavage. Fabric is partitioned in coarser quartzofeldspathic psammitic beds, producing normal-to-bed spaced fracture cleavage, while pelitic and semipelitic beds promote near-parallel penetrative biotite foliation fabric. Beds are overturned with tops to the right in south-verging sequence.

**Figure 5.** Perspective view of an interpretation that extends Bravo Lake Formation, mafic volcanic klippen along the section line. Section plane cuts topography along thin green line in north-south direction. Note that thickness estimate of the mafic unit is unconstrained. One kilometre structural-contour interval. Perspective view looking northeast.





**Figure 6.** Preliminary 3D interpretation of fault surface below Bravo Formation mafic volcanic rocks southwest of Nadluardjuk Lake. Perspective view looking northeast. For methodology used in constructing 3D surface models see de Kemp and Sprague (2001).

**Table 1.** Structural history.

Deformation Event	Basement Archean gneiss, granitoid	Cover (Piling Group)	Paleoproterozoic granitoid, southern and northern	General orientation
D <sub>1A</sub> *	Unknown			SW-NE
D <sub>1P</sub>	Unknown	Thrusting/transposition/folding		E-W
D <sub>2P</sub>	Tight to isoclinal F <sub>2</sub>	Upright isoclinal F <sub>2</sub> tightening of F <sub>1</sub>	Upright F <sub>2</sub> , transposition	ENE-WSW
D <sub>3P</sub>	Open F <sub>3</sub>	Open F <sub>3</sub>	Open F <sub>3</sub>	NW-SE
A = Archean, P = Paleoproterozoic				